

Investigating Short-Term Dynamics in Green Bond Markets

Lorenzo Mercuri

Department of Economics Management and Quantitative Methods, University of Milan, Milan, Italy
email: lorenzo.mercuri@unimi.it

Andrea Perchiazzo

Faculty of Economics and Social Sciences and Solvay Business School, Vrije Universiteit Brussel, Brussels, Belgium
email: andrea.perchiazzo@vub.be

Edit Rroji

Department of Statistics and Quantitative Methods, University of Milano-Bicocca, Milan, Italy
email: edit.rroji@unimib.it

Abstract

The paper investigates the effect of the label green in bond markets from the lens of the trading activity. The idea is that jumps in the dynamics of returns have a specific memory nature that can be well represented through a self-exciting process. Specifically, using Hawkes processes where the intensity is described through a continuous time moving average model, we study the high-frequency dynamics of bond prices. We also introduce a bivariate extension of the model that deals with the cross-effect of upward and downward price movements. Empirical results suggest that differences emerge if we consider periods with relevant interest rate announcements, especially in the case of an issuer operating in the energy market.

Keywords: Green Bond, Jumps, Self-exciting

Introduction

In recent years the pressure of solutions for the environment (e.g., transition to a lower-carbon economy, energy efficiency, and construction of renewable source plants) has solicited the need of alternative funding. A clear example is the creation of a financial instrument called green bond, which is used exclusively to raise money for financing environmental (labeled as “green”) projects. Following the principles of the International Capital Markets Association (ICMA) some categories of these investments funded through green bonds are destined to renewable energy, green buildings, public transport, energy efficiency, water, and waste management.

A topic of interest in the financial literature is the “greenium” (or “green” premium) effect, which refers to the fact that bondholders are willing to pay a higher price or accept a lower yield in order to invest in green securities compared to conventional securities with similar characteristics (e.g., maturity, coupon rate, and credit profile of the issuer).

Several papers have tried to identify the main factors that drive the “greenium” effect with particular emphasis on the issuer (that is, differentiating corporate, municipal, and sovereign bonds). Hereafter, we list some findings. [1] do not find significant differences between the yield of green and conventional bonds with the same issuer; whereas, for example, [2] find that the type of bond issuer (i.e., institutional versus private) is relevant in order to detect the “greenium” effect. In addition to that, [3] claim that US corporate and municipal green-labeled bonds are issued above par (that is, at premium) with respect to non-green-labeled bonds, while [4] and [5] show that green bonds provide diversification benefits to portfolios. Moreover, [6] suggest that portfolios with green bonds are less risky through time for different allocation strategies. [7] show that the co-movements between green-labeled and non-green-labeled markets are more pronounced in the short-term horizon.

Previous literature is mainly based on panel regressions that consider weekly or daily data (see for example [8]) in which contract-specific or general macroeconomic variables are included as explanatory variables. Green bonds started to be issued in European Union only in the last decade when interest rates were low or negative for a long period of time and, consequently, the existing literature refers to markets with those conditions. In this paper, we propose a different viewpoint as we consider the intraday dynamics of bond returns where jumps are potentially explained through some market announcements.

Focusing on the high frequency framework, classical bonds have been widely investigated in the literature (see, for instance, [9] and [10]) whereas, at the best of our knowledge, a study on green bonds has not been taken under consideration yet. In this paper, we analyze the effect of the label green by looking at returns computed on tick data and we propose a procedure for the investigation of the impact news in the market may have on the time series of bond prices. In particular, we use the Lee and Mykland’s (LM) test (see [11] for further details) for the identification of jumps. The framework presented in the paper can be generalized by considering alternative tests for jump detection, see for example [12] for a list of non-parametric tests.

Jumps are important in finance from different points of view. For example [13] show how to price Asian options in presence of jump clusters while [14] show that jumps significantly affect future realized volatility and used them for oil futures volatility prediction. Our analysis is based on a counting process, proposed in [15], where the conditional intensity is modelled with the continuous version of the ARMA process called a CARMA(p,q)-Hawkes. Such a model implies a self-exciting behaviour with a non monotone autocorrelation function for jumps in non-overlapping intervals of the same length. We expect some particular market conditions to generate different sequences of jumps for pairs of brown and green bonds with similar features in terms of credit quality, coupon rate, duration, and currency. As a set of jumps defines a point process, then by distinguishing between positive and negative jumps it is possible to consider a bivariate point process. To this aim, we introduce the bivariate version of the CARMA(p,q)-Hawkes model and present an estimation procedure. In our empirical analysis, we consider two periods each of length

one month. In the first period (from August 19 to September 19, 2022) the market dealt with an announcement of the European Central Bank (ECB) on the interest rate raise while in the second period (from November 14 to December 13, 2022) the market had no announcements from ECB but it experienced a particularly nervous moment due to the uncertainty in gas price in Europe. Issuers are two companies that operate in the European market. The first is the financial institution Crédit Agricole SA while the second issuer, which is a corporate company operating in the energy sector issuing both green and brown bonds, is Engie SA.¹

This paper attempts to shed light on differences that emerge in terms of market activity and liquidity for different bond redemption types, market sector of the issuer and currency.

In our analyses, bid prices display more jumps for the series considered. We also observe that higher order CARMA(p,q)-Hawkes seems to be useful for the series of jumps extracted from the returns of the bonds issued by the corporate company operating in the energy sector.

The paper is organized as follows. Section 1 introduces the bivariate CARMA(p,q)-Hawkes model. Section 2 presents the likelihood function of the bivariate CARMA(p,q)-Hawkes model, the different frameworks under investigation and the description of the estimation procedure. Section 3 shows the empirical results. Section 4 concludes the paper.

1. Self-exciting processes

We briefly review classical counting processes and discuss the main features of a CARMA(p,q)-Hawkes model² (see [15] for a complete overview) that is an extension of the Hawkes type processes where the effect of past realizations is not monotonically decreasing, see [16] for an overview of Hawkes processes in finance. In order to investigate the cross effect of positive and negative jumps in the series of bond returns we introduce the bivariate CARMA(p,q)-Hawkes model.

1.1. Hawkes-type processes

A point process, which is used to describe the dynamics of observed event times, is a collection of realizations $\{t_i\}_{i=1}^{\infty}$ where $t_0 := 0$ and $t_i \geq 0$ for $i = 1, 2, \dots$ of the non-decreasing and non-negative process $\{T_i\}_{i \geq 1}$ (i.e., the time arrival process). The counting process N_t , representing the number of events up to time t and obtained from the time arrival process, is defined as

$$N_t := \sum_{i \geq 1} \mathbf{1}_{\{T_i \leq t\}} \quad (1)$$

¹Engie SA is the largest non sovereign green bond issuer in France.

²As highlighted in [15], an exponential Hawkes process shows a strictly decreasing behaviour of the autocorrelation function. In order to remove such a monotonicity constraint, it is possible to consider a Hawkes process where the intensity follows a CARMA process that can provide several shapes of the autocorrelation function. The latter is an extension of the classical Hawkes model.

for $t \geq 0$ with associated filtration $(\mathcal{F}_t)_{t \geq 0}$, which contains the information of N_t . In practice, if we look at a series of returns the point process refers to the sequence of time events while the counting process to the number of jumps occur up to a fixed time instant t . The conditional intensity λ_t for the counting process N_t is defined as

$$\lambda_t = \lim_{\Delta \rightarrow 0^+} \frac{\Pr[N_{t+\Delta} - N_t = 1 | \mathcal{F}_t]}{\Delta},$$

and straightforwardly follows that the counting process satisfies

$$\Pr[N_{t+\Delta} - N_t = \eta | \mathcal{F}_t] = \begin{cases} 1 - \lambda_t \Delta + o(\Delta) & \text{if } \eta = 0 \\ \lambda_t \Delta + o(\Delta) & \text{if } \eta = 1 \\ o(\Delta) & \text{if } \eta > 1. \end{cases}$$

The conditional intensity λ_t of a general self-exciting process has the following form

$$\lambda_t = \mu + \int_0^t h(t-s) dN_s \quad (2)$$

with baseline intensity parameter $\mu > 0$ and kernel function $h(t) : [0, +\infty) \rightarrow [0, +\infty)$, representing the contribution to the intensity at time t made by an event occurred at a previous time $T_i < t$. Note that the condition of stationarity is given by $\int_0^{+\infty} h(t) dt < 1$. The case of the exponential kernel, i.e. $h(t) = \alpha e^{-\beta t}$ with $\alpha, \beta \geq 0$, defines the classical Hawkes model where the long-run autocorrelation function of the number of jumps over intervals of length τ separated by a time lag of δ has the following characteristics: i) is strictly monotonic decreasing function of δ (see [17] for further details), ii) is always positive for $\alpha < \beta$ (stationarity condition), and iii) is exponentially decaying with lag δ . The use of the continuous autoregressive moving average models for the conditional dynamics of λ_t generalizes the classical Hawkes with the advantage of reproducing different shapes of the autocorrelation function.

1.2. CARMA(p,q)-Hawkes process

A $(p+1)$ vector process $[X_{1,t}, \dots, X_{1,p}, N_t]^\top$ is classified as a CARMA(p,q)-Hawkes process if the conditional intensity λ_t of the counting process N_t takes the form of a CARMA(p,q) process driven by N_t , characterized as follows

$$\lambda_t = \mu + \mathbf{b}^\top X_t. \quad (3)$$

μ is the positive baseline intensity, and $\mathbf{b} = [b_0, b_1, \dots, b_{p-1}]^\top$ with $b_{q+1} = \dots = b_{p-1} = 0$ contains the moving average parameters. The vector $X_t = [X_{1,t}, \dots, X_{1,p}]^\top$ satisfies the subsequent linear

stochastic differential equation

$$dX_t = \mathbf{A}X_t dt + \mathbf{e}dN_t \text{ with } X_0 = \mathbf{0}, \quad (4)$$

where $\mathbf{e} = [0, 0, \dots, 1]^\top$ and the matrix \mathbf{A} is defined as

$$\mathbf{A} = \begin{bmatrix} 0 & 1 & 0 & \dots & 0 \\ 0 & 0 & 1 & \dots & 0 \\ \vdots & \vdots & \vdots & \ddots & \vdots \\ 0 & 0 & 0 & \dots & 1 \\ -a_p & -a_{p-1} & -a_{p-2} & \dots & -a_1 \end{bmatrix}_{p \times p}, \quad (5)$$

where (a_1, \dots, a_p) are the autoregressive parameters.

The stochastic differential equation in (4) admits an analytical solution given the initial condition, which reads:

$$X_t = \int_0^t e^{\mathbf{A}(t-s)} \mathbf{e} dN_s. \quad (6)$$

We now provide an overview of the likelihood function for the CARMA(p,q)-Hawkes process (for detailed insights, refer to [15, Section 4.2]) that we will use in the empirical analysis. Given observed time arrivals T_1, \dots, T_n , the likelihood function is expressed as

$$\mathcal{L}(\theta) = -\mu T_n - \mathbf{b}^\top \mathbf{A}^{-1} S(n) \mathbf{e} + n \mathbf{b}^\top \mathbf{A}^{-1} \mathbf{e} + \sum_{i=1}^n \ln(\lambda_{T_i}),$$

where $S(n) = \sum_{i=1}^n e^{\mathbf{A}(T_n - T_i)}$.

The stationarity conditions for the CARMA(p,q)-Hawkes, ensuring a non-negative kernel, and establishing the diagonalizability of matrix \mathbf{A} are discussed in [15]. The same paper also offers a simulation algorithm and an alternative estimation procedure based on the autocorrelation function of the number of jumps observed in two non-overlapping intervals of equal length.

1.3. Bivariate CARMA(p,q)-Hawkes process

Let N_t^+ and N_t^- denote respectively the number of upward and downward jumps in the time interval $[0, t]$. The bivariate version of a CARMA(p,q)-Hawkes process imposes a cross-dependence between the upward and downward jump intensities respectively named $\lambda_{t,1}$ and $\lambda_{t,2}$. As the number of parameters increases in the bivariate case, we introduce the following quantities for sake of clarity in the model description:

- i) let $\mathbf{p} := [p_1, p_2]$ be the dimension of the autoregressive parameters where p_1 and p_2 are respectively the dimensions of the state processes $X_{t,1}$ and $X_{t,2}$;
- ii) let $\mathbf{q} := [q_1, q_{1,2}, q_{2,1}, q_2]$ be the dimension of the moving average parameters;

- iii) let $\mathbf{b}_{1,1} := [b_{1,1}^{(0)}, \dots, b_{1,1}^{(p_1-1)}]^\top$ with $b_{1,1}^{(q_1+1)} = \dots = b_{1,1}^{(p_1-1)} = 0$ be a column vector of dimension $p_1 \times 1$;
- iv) let $\mathbf{b}_{1,2} := [b_{1,2}^{(0)}, \dots, b_{1,2}^{(p_2-1)}]^\top$ with $b_{1,2}^{(q_1,2+1)} = \dots = b_{1,2}^{(p_2-1)} = 0$ be a column vector of dimension $p_2 \times 1$;
- v) let $\mathbf{b}_{2,1} := [b_{2,1}^{(0)}, \dots, b_{2,1}^{(p_1-1)}]^\top$ with $b_{2,1}^{(q_2,1+1)} = \dots = b_{2,1}^{(p_1-1)} = 0$ be a column vector of dimension $p_1 \times 1$;
- vi) let $\mathbf{b}_{2,2} := [b_{2,2}^{(0)}, \dots, b_{2,2}^{(p_2-1)}]^\top$ with $b_{2,2}^{(q_2+1)} = \dots = b_{2,2}^{(p_2-1)} = 0$ be a column vector of dimension $p_2 \times 1$.

The intensities of N_t^+ and N_t^- , respectively $\lambda_{t,1}$ and $\lambda_{t,2}$, are modelled as

$$\begin{aligned}\lambda_{t,1} &= \mu_1 + \mathbf{b}_{1,1}^\top X_{t,1} + \mathbf{b}_{1,2}^\top X_{t,2} \\ \lambda_{t,2} &= \mu_2 + \mathbf{b}_{2,1}^\top X_{t,1} + \mathbf{b}_{2,2}^\top X_{t,2}\end{aligned}\tag{7}$$

where

$$\begin{aligned}dX_{t,1} &= \mathbf{A}_1 X_{t,1} dt + \mathbf{e}_1 dN_t^+ \\ dX_{t,2} &= \mathbf{A}_2 X_{t,2} dt + \mathbf{e}_2 dN_t^-\end{aligned}\tag{8}$$

It is worth to note that \mathbf{A}_1 , \mathbf{A}_2 , \mathbf{e}_1 , and \mathbf{e}_2 have the same structure of the corresponding \mathbf{A} and \mathbf{e} denoted in Section 1.2.

Then $\mathbf{N}_t := [N_t^+ \ N_t^-]^\top$ is a bivariate self-exciting counting process with intensity process $\boldsymbol{\lambda}_t = [\lambda_{t,1} \ \lambda_{t,2}]^\top$. It is possible to simplify the notation using the following quantities

$$\boldsymbol{\mu} = \begin{bmatrix} \mu_1 \\ \mu_2 \end{bmatrix}, \quad \mathbf{B} = \begin{bmatrix} \mathbf{b}_{1,1}^\top & \mathbf{b}_{1,2}^\top \\ \mathbf{b}_{2,1}^\top & \mathbf{b}_{2,2}^\top \end{bmatrix}_{2 \times (p_1+p_2)} \quad \text{and} \quad \mathbf{X}_t = \begin{bmatrix} X_{t,1} \\ X_{t,2} \end{bmatrix} \in \mathbb{R}^{p_1+p_2}.$$

Indeed, the bivariate CARMA(p,q)-Hawkes process reads

$$\boldsymbol{\lambda}_t = \boldsymbol{\mu} + \mathbf{B}\mathbf{X}_t\tag{9}$$

and

$$d\mathbf{X}_t = \bar{\mathbf{A}}\mathbf{X}_t dt + \bar{\mathbf{e}} d\mathbf{N}_t, \quad \text{with } X_0 = 0,$$

where

$$\bar{\mathbf{A}} = \begin{bmatrix} \mathbf{A}_1 & 0 \\ 0 & \mathbf{A}_2 \end{bmatrix} \quad \text{and} \quad \bar{\mathbf{e}} = \begin{bmatrix} \mathbf{e}_1 & 0 \\ 0 & \mathbf{e}_2 \end{bmatrix}_{(p_1+p_2) \times 2}.$$

We remark that the state process of $\boldsymbol{\lambda}_t$ in (9) is still a linear stochastic differential equation where the driving noise is a bivariate counting process and has an analytical solution.

The likelihood of the bivariate CARMA(p,q)-Hawkes process, where $\theta = (\boldsymbol{\mu}, \bar{\mathbf{A}}, \mathbf{B})$ contains the

set of parameters to estimate, reads

$$\mathcal{L}(\theta) = \sum_{i=1}^2 \left[- \int_0^T \lambda_{t,i} dt + \int_0^T \ln(\lambda_{t,i}) dN_{t,i} \right]. \quad (10)$$

Let us denote $\mathbb{1} = [1 \ 1]^\top$ and $\ln(\boldsymbol{\lambda}_t) = [\ln(\lambda_{t,1}) \ \ln(\lambda_{t,2})]^\top$, then (10) can be rewritten as

$$\mathcal{L}(\theta) = - \int_0^T \mathbb{1}^\top \boldsymbol{\lambda}_t dt + \int_0^T \ln(\boldsymbol{\lambda}_t)^\top d\mathbf{N}_t. \quad (11)$$

Substituting (9) in (11) and making some calculations, we finally get

$$\begin{aligned} \mathcal{L}(\theta) &= - \int_0^T \mathbb{1}^\top [\boldsymbol{\mu} + \mathbf{B}\mathbf{X}_t] dt + \int_0^T \ln(\boldsymbol{\mu} + \mathbf{B}\mathbf{X}_t)^\top d\mathbf{N}_t \\ &= - \mathbb{1}^\top \boldsymbol{\mu} (T - 0) - \mathbb{1}^\top \mathbf{B} \int_0^T \mathbf{X}_t dt + \sum_{T_k \leq T} \ln(\boldsymbol{\mu} + \mathbf{B}\mathbf{X}_{T_k})^\top \Delta \mathbf{N}_{T_k} \end{aligned} \quad (12)$$

where $\Delta \mathbf{N}_{T_k} := \mathbf{N}_{T_n} - \mathbf{N}_{T_k-}$ and \mathbf{N}_{T_k-} is the left limit of the bivariate process. Note that $\Delta \mathbf{N}_{T_k} = [1 \ 0]^\top$ (or equivalently $[0 \ 1]^\top$) where T_k is the bivariate jump time process; specifically, $T_k = [T_{k,1} \ T_{k,2}]^\top$.

Recalling that $\bar{\mathbf{e}}$ is a $(p_1 + p_2) \times 2$ matrix with zero elements, except for $\mathbf{e}_{p_1,1} = 1$ and $\mathbf{e}_{(p_1+p_2),2} = 1$, we consider the following summation defined iteratively as

$$\begin{aligned} s(1) &= \bar{\mathbf{e}} \Delta \mathbf{N}_{T_1} \\ s(n) &= \bar{\mathbf{e}} \Delta \mathbf{N}_{T_n} + e^{\bar{\mathbf{A}}(T_n - T_{n-1})} s(n-1). \end{aligned}$$

Assuming that $T = T_n$ (i.e., we have n jumps in $[0, T_n]$), the likelihood function of the bivariate CARMA(p,q)-Hawkes finally becomes

$$\mathcal{L}(\theta) = - \mathbb{1}^\top \boldsymbol{\mu} T_n + \mathbb{1}^\top \mathbf{B} \bar{\mathbf{A}}^{-1} \mathbf{e} \mathbf{N}_{T_n} - \mathbb{1}^\top \mathbf{B} \bar{\mathbf{A}}^{-1} s(n) + \sum_{i=1}^n \ln(\boldsymbol{\mu} + \mathbf{B}\mathbf{X}_{T_i})^\top \Delta \mathbf{N}_{T_i}. \quad (13)$$

See Appendix A for the derivation of (13).

2. Description of the estimation procedure

The estimation exercise presented in the paper is based on an iterative sequential procedure which considers three different frameworks: the bivariate CARMA(p,q)-Hawkes (bCH) framework applied directly to the series of upward and downward price movements, the univariate CARMA(p,q)-Hawkes combined with the Lee and Mykland test for jump detection (hereafter uCHLM framework), and the bivariate CARMA(p,q)-Hawkes with Lee and Mykland test (bCHLM

framework). We first discuss the test of Lee and Mykland (hereafter LM test) proposed in [11] and then dive into the details of the considered frameworks.

Let $P(t_i)$ be the asset price at time t_i for $i = 1, \dots, n$. In the LM test, the quantity $\mathcal{M}(i)$, is defined as

$$\mathcal{M}(i) := \frac{\log \frac{P(t_i)}{P(t_{i-1})}}{\hat{\sigma}^2(t_i)}, \quad (14)$$

with $\hat{\sigma}^2(t_i)$ given by

$$\hat{\sigma}^2(t_i) := \frac{1}{K-2} \sum_{j=i-K+2}^{i-1} \left| \log \frac{P(t_j)}{P(t_{j-1})} \right| \left| \log \frac{P(t_{j-1})}{P(t_{j-2})} \right|,$$

where K is the window size. Note that (14) tests at time t_i if a jump happened in the time interval from t_{i-1} to t_i . Here we state the following asymptotic result based on [11, Lemma 1], assuming zero drift for the dynamics of P_t in but in the *highfrequency* R package described in [18] the LM test is implemented also in the case with possible non zero drift term.

Let be $K = O_p(\Delta t^{\bar{\alpha}})$ where $-1 < \bar{\alpha} < -0.5$ and assume zero drift for the dynamics of P_t , then as $\Delta t \rightarrow 0$

$$\frac{\mathcal{M}(i) - C_n}{S_n} \rightarrow \eta \quad (15)$$

where η has a cumulative distribution function $P(\eta \leq x) = \exp(-e^{-x})$. The quantities C_n and S_n are respectively

$$C_n = \frac{(2 \log n)^{1/2}}{c} - \frac{\log \pi + \log(\log n)}{2c(2 \log n)^{1/2}} \quad \text{and} \quad S_n = \frac{1}{c(2 \log n)^{1/2}},$$

where n denotes the number of observations and $c \approx 0.7979$. In this paper we use the LM test for detecting the jumps within an intraday data set, but other tests can be considered for the detection of jumps. For instance, a list of non-parametric tests for detecting jumps presented in [12] can be used in order to extend the proposed analyses.

2.1. Frameworks under investigation

Here we present the frameworks under investigation and we recall that we look for the autoregressive and moving average orders of CARMA(p,q)-Hawkes models (univariate or bivariate). The main difference of the frameworks under investigation refers to the data we give as input to the model to be fitted, i.e. the definition of jumps. The three frameworks are sequential since if one fails to be accepted (see Section 2.2 for the type of test), then the algorithm moves on to the next one.

1. **The bCH framework** In this framework any price movement is used to define N_T^+ and N_T^- that refer respectively to the sequence of positive and negative price movements (i.e., $\mathbf{N}_t = [N_T^+ \ N_T^-]^\top$ is a bivariate point process where the intensities are defined in (9)).

2. **The uCHLM framework.** Here, we consider the univariate CARMA(p,q)-Hawkes model fitted to the univariate vector N_T that contains jumps which in this context refer to the abnormal price movements. Jumps are identified by means of the LM test. Four different levels of confidence intervals for the LM test are considered, namely $\alpha_{LM} \in \{95\%, 97.5\%, 99\%, 99.5\%\}$.
3. **The bCHLM framework.** Similar to the bCH framework, but, in this case, we consider the vector of jumps detected through the LM test by distinguishing between positive and negative jumps. In practice, we repeat the whole procedure applied to the newly defined vector $\mathbf{N}_t = [N_T^+ \ N_T^-]^\top$ for $\alpha_{LM} \in \{95\%, 97.5\%, 99\%, 99.5\%\}$.

2.2. Routine of the estimation procedure

The estimation procedure for the analysis starts from the simplest model (i.e., the bCH framework); see the diagram in Figure B.5. Then it proceeds with the estimation phase (yellow box) in which two models are fitted: the candidate and the alternative models. Such estimation is based on the maximization of the likelihood function. Once obtained the optimal parameters, a model selection between the candidate and alternative models is performed (red box).

In case of non-nested models the model selection exploits the Akaike information criterion (AIC) while in case of nested models, model selection is based on the likelihood-ratio (LR) test. In traditional statistical theory, such a test is widely accepted for testing the goodness of fit between nested models. The statistic of the likelihood ratio test, i.e., LR , can be computed as the difference of two loglikelihoods in nested models. Specifically,

$$LR = 2 (\log \mathcal{L}^{\text{unrest.}}(\theta) - \log \mathcal{L}^{\text{rest.}}(\theta)). \quad (16)$$

is asymptotically distributed as a χ^2 with degrees of freedom equal to the number of additional parameters in the unrestricted model (see [19] for further details). For sake of clarity, we provide an example. Suppose that we choose for the candidate model (bCH framework), which is the restricted one, the following orders $\mathbf{p} = [1, 1]$ and $\mathbf{q} = [0, 0, 0, 0]$. For the alternative model, which is the unrestricted one, a natural choice is to consider the model with $\mathbf{p} = [2, 1]$ and $\mathbf{q} = [1, 0, 1, 0]$. In case of rejection of the null hypothesis, we consider a new unrestricted model³ (i.e., a new alternative model); for instance, a larger combination of orders such as $\mathbf{p} = [2, 2]$ and $\mathbf{q} = [1, 1, 1, 1]$. Thus the idea, in case of rejection of the null hypothesis, is keep testing nearby models until the null hypothesis fails to be rejected. Note that, considering nested and non-nested model, the routine generates four possible scenarios (see green box of Figure B.5). Two scenarios refer to the possibility that there is at least an alternative or nearby model to verify while the other two concern the case in which there are no alternative or nearby models. If that is the situation, then the optimal orders

³At this stage the alternative model becomes the candidate model.

of that framework are identified. After the identification of the best fitting model, the algorithm moves on to the next step which is the *residual analysis*. Such an analysis is used to establish whether the data are generated by the selected model and works as follows. Let us suppose that the observed time arrivals $\{t_i\}_{i=1,\dots,n}$ are generated by the conditional intensity λ_t . Then we construct a new set of time arrivals $\{\tau_i\}_{i=1,\dots,n}$, as follows:

$$\tau_i := \int_0^{t_i} \lambda_t dt. \quad (17)$$

The transformed data τ_i are expected to follow a stationary Poisson process with unitary intensity (see for example [20] for details) and can be used to test the form of the conditional intensity. In our routine we implement the Kolmogorov-Smirnov (KS) test, which tests the residual differences between the empirical and theoretical cumulative distribution functions of the inter-event (or inter-arrival) times. Specifically, inter-event times are denoted as

$$u_i := \tau_i - \tau_{i-1},$$

with $\tau_0 = 0$. If λ_t is correctly specified (i.e., λ_t is positive over $[0, T]$ and $\int_0^T \lambda_t dt < \infty$ a.s.), then $\{u_i\}_{i=1,\dots,n}$ are i.i.d. exponentially distributed with unit rate. If the identified model does not pass the residual analysis, then the algorithm moves on to the next framework. If the opposite happens, then the procedure identifies the best model and stops. Figure B.5 displays an overview of the routine.

3. Empirical Analysis

3.1. Descriptive analysis

In this section we discuss the results of the estimation and the selection procedure previously described conducted on different bonds issued by Cr dit Agricole SA (financial institution issuing green bonds since 2013) and Engie SA (corporate company operating in the energy market, the largest non sovereign green bond issuer in France) observed in two different time periods. The main assumption is that in summer and in autumn the news in the energy market are quite relevant for highlighting differences in green and brown bonds. Moreover, we deal with two time frameworks where there is a difference based on whether the ECB made interest rate announcements or not. The data refer to tick data (ask and bid prices) downloaded from Bloomberg where we consider the Green label indicator. The first period ranges from August 19 to September 19, 2022 while the second period ranges from November 14 to December, 2022. For Cr dit Agricole we consider two types of bonds (bullet and callable) while for Engie only bullet bonds. We select pairs of bonds (green and brown) with similar maturity, coupon rate, currency and rating.

The main features of these instruments are reported in Table 1 while in Tables 2 and 3 we present

the main statistics of the bid-ask spread for the three groups (green and brown bonds) for two high frequency data with time window length equal to one month. It results that the observed bid-ask spread of green bonds on average is larger for green bonds issued by Cr dit Agricole SA, especially in the second time period. The opposite happens for the bonds issued by Engie SA. For the callable bonds issued by Cr dit Agricole SA the results are mixed. Indeed, the currency of these bond is the Singapore Dollar (SGD) and there are quotations only for the half trading day. It clearly emerges that some intraday news are absorbed with a different time lag with respect to the series of bonds quoted in the European market. We also highlight the fact that bid-ask spreads for the bullet bonds (green and brown) do not display significant differences in the two non-overlapping time intervals while for the case of the callable bonds we observe on average larger values and standard deviation in the case of the green instrument.

| Bullet | | | | | | | |
|------------------|------------|--------|--------|------------|----------|-----------|-------|
| Coupon | Maturity | Series | Rating | Announce | Currency | Ask Price | Type |
| 0.375 | 21/10/2025 | EMTN | A- | 14/10/2019 | EUR | 92.611 | Green |
| 0.5 | 24/06/2024 | EMTN | A- | 17/06/2019 | EUR | 96.344 | Brown |
| Callable | | | | | | | |
| Coupon | Maturity | Series | Rating | Announce | Currency | Ask Price | Type |
| 3.95 | 22/07/2032 | EMTN | BBB+ | 13/04/2022 | SGD | 97.697 | Green |
| 3.8 | 30/04/2031 | EMTN | BBB+ | 23/04/2019 | SGD | 98.364 | Brown |
| Bullet Corporate | | | | | | | |
| Coupon | Maturity | Series | Rating | Announce | Currency | Ask Price | Type |
| 0.875 | 27/03/2024 | EMTN | BBB+ | 15/03/2017 | EUR | 97.481 | Green |
| 0.375 | 11/06/2027 | EMTN | BBB+ | 04/06/2020 | EUR | 87.163 | Brown |

Table 1: Features of bonds included in the dataset. The issuers are Cr dit Agricole SA (financial) and Engie SA (corporate). Prices refer to September 19, 2022.

| Aug-Sep | Mean | Med. | Mode | Std. | Ex. Kur. | Skew. | IQR | Min | Max |
|-------------------------|--------|--------|--------|--------|----------|---------|--------|--------|--------|
| Bullet Fin (G) | 0.2650 | 0.2640 | 0.2560 | 0.0113 | 0.1904 | 0.1945 | 0.1080 | 0.2230 | 0.3310 |
| Bullet Fin (B) | 0.1987 | 0.1970 | 0.1910 | 0.0111 | 0.2999 | 0.5853 | 0.1070 | 0.1630 | 0.2700 |
| Callable Fin (G) | 0.8193 | 0.8180 | 0.7650 | 0.2350 | -0.7506 | 0.3930 | 0.2300 | 0.7210 | 0.9510 |
| Callable Fin (B) | 0.8869 | 0.8230 | 0.7880 | 0.2342 | 12.6908 | 3.6924 | 1.7220 | 0.7470 | 2.4690 |
| Bullet Corp (G) | 0.2374 | 0.2390 | 0.2440 | 0.0302 | -0.8252 | -0.0418 | 0.0491 | 0.1710 | 0.350 |
| Bullet Corp (B) | 0.3677 | 0.3660 | 0.3360 | 0.0279 | -0.3826 | 0.6439 | 0.0430 | 0.2990 | 0.4460 |

Table 2: Main statistics of the bid-ask spread for the bonds included in the dataset. The label in brackets refers to the bond's type G for green and B for brown. The data refer to the period August 19 - September 19, 2022.

| Nov-Dec | Mean | Med. | Mode | Std. | Ex. Kur. | Skew. | IQR | Min | Max |
|-------------------------|-------------|-------------|-------------|-------------|-----------------|--------------|------------|------------|------------|
| Bullet Fin (G) | 0.2869 | 0.2860 | 0.2830 | 0.0094 | 0.6992 | 0.4862 | 0.0770 | 0.2580 | 0.3350 |
| Bullet Fin (B) | 0.1854 | 0.1830 | 0.1790 | 0.0102 | -0.2050 | 0.5818 | 0.0660 | 0.1560 | 0.2220 |
| Callable Fin (G) | 2.9652 | 3.0610 | 3.4090 | 0.3837 | 0.2112 | -0.8960 | 1.4180 | 2.0890 | 3.5070 |
| Callable Fin (B) | 1.5423 | 1.5000 | 1.4990 | 0.1841 | -1.0681 | -0.0598 | 0.6380 | 1.2010 | 1.8390 |
| Bullet Corp (G) | 0.2709 | 0.2680 | 0.2620 | 0.0191 | 0.2792 | 0.461 | 0.0260 | 0.2130 | 0.3441 |
| Bullet Corp (B) | 0.3463 | 0.3610 | 0.3690 | 0.0212 | -0.8068 | -0.1887 | 0.0360 | 0.3090 | 0.4270 |

Table 3: Main statistics of the bid-ask spread for the bonds included in the dataset. The label in brackets refers to the bond's type G for green and B for brown. The data refer to the period November 14 - December 13, 2022.

3.2. Analysis of the microstructure based on jumps

In this section we present the main results from the fitting of the univariate and bivariate CARMA(p,q)-Hawkes model introduced in Section 2.1. As the three frameworks under consideration require an underlying point process we consider the LM test for the jump identification. Indeed, for each series (bid and ask) we identify four sequences of jumps as we vary the confidence level of the LM test ($\alpha_{LM} \in \{0.95, 0.975, 0.99, 0.995\}$). For each value of α_{LM} we compute the percentage of observations classified as jumps. Data refer to intraday bid and ask prices.

Differences emerge both by looking at different bond types and different points in time. For example, Figures 1 and 2 refer to prices and returns of respectively the green and the brown bonds issued by Crédit Agricole SA (included in the dataset) observed at September 8, 2022. At this date, at 14:45 the ECB announced an increase in the reference interest rate. Both series (bid and ask) experienced a drop in the price value immediately after the ECB announcement. The same quantities for November 22, 2022 are displayed respectively in Figures 3 and 4. Similar plots for callable bonds issued by Crédit Agricole SA and bullet bonds issued by Engie SA are reported in Appendix C. In particular Figures C.6 and C.7 provide information on the set of callable bonds at September 8, 2022 while C.8 and C.9 at November 22, 22. For the bonds issued by Engie SA we refer to Figures C.10 and C.11 for data observed at September 8, 20022 and to Figures C.12 and C.13 for November 22, 2022.

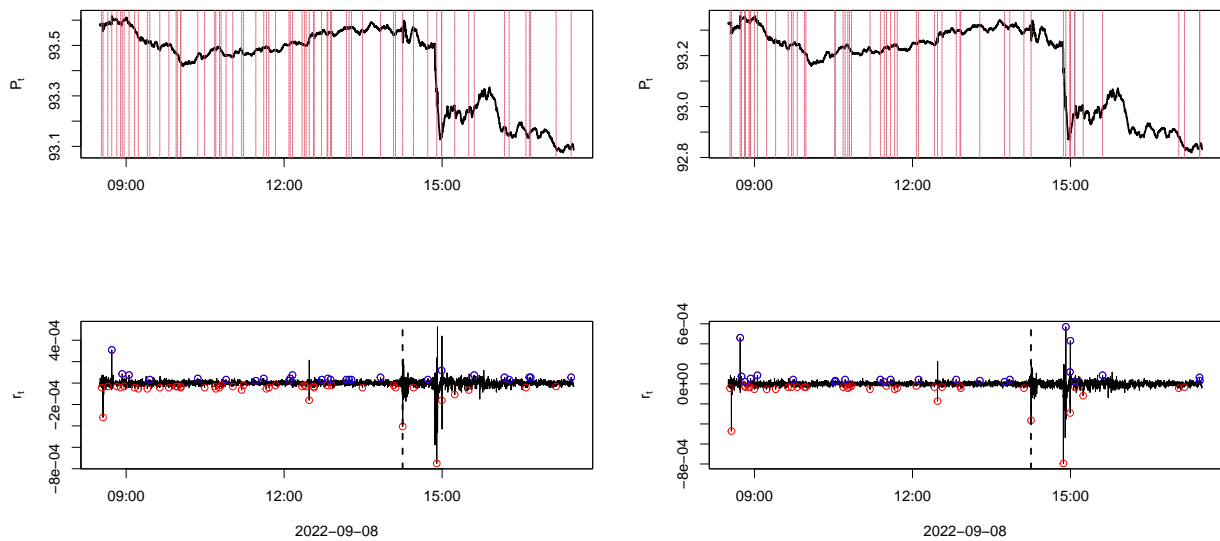


Figure 1: Prices and returns of the green bullet bond issued by Crédit Agricole SA observed at September 8, 2022 (plots on the left refer to ask prices/returns while plots on the right to the bid counterparts). Red and blue circles refer respectively to negative and positive jumps in the series of returns identified through the LM test for $\alpha_{LM} = 0.95$. Vertical red lines in the upper plots refer to time instants where (positive or negative) jumps occur.

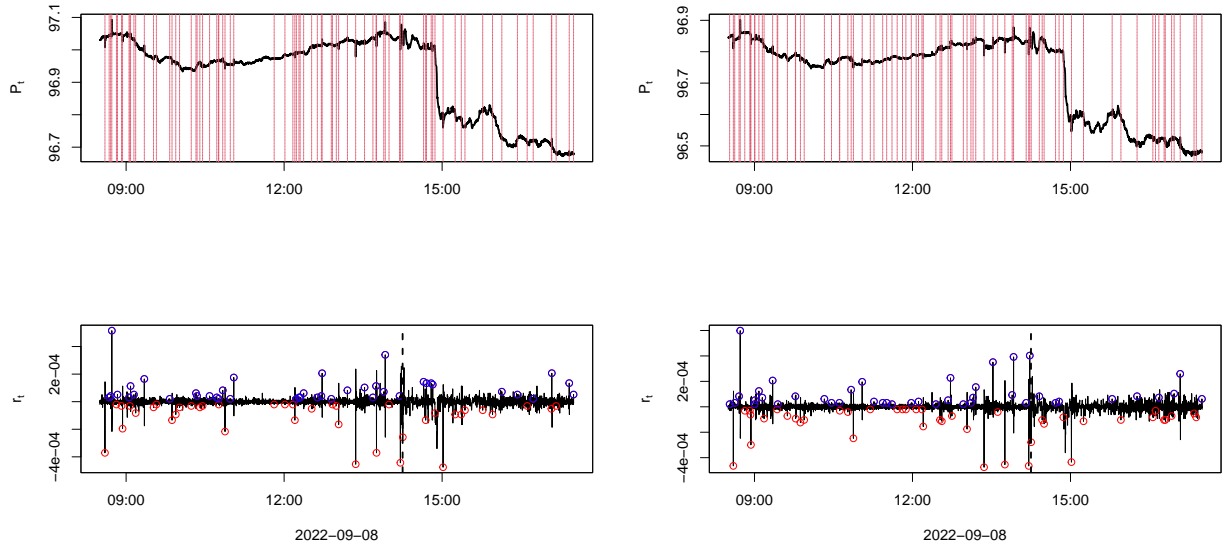


Figure 2: Prices and returns of the brown bullet bond issued by Crédit Agricole SA observed at September 8, 2022 (plots on the left refer to ask prices/returns while plots on the right to the bid counterparts). Red and blue circles refer respectively to negative and positive jumps in the series of returns identified through the LM test for $\alpha_{LM} = 0.95$. Vertical red lines in the upper plots refer to time instants where (positive or negative) jumps occur.

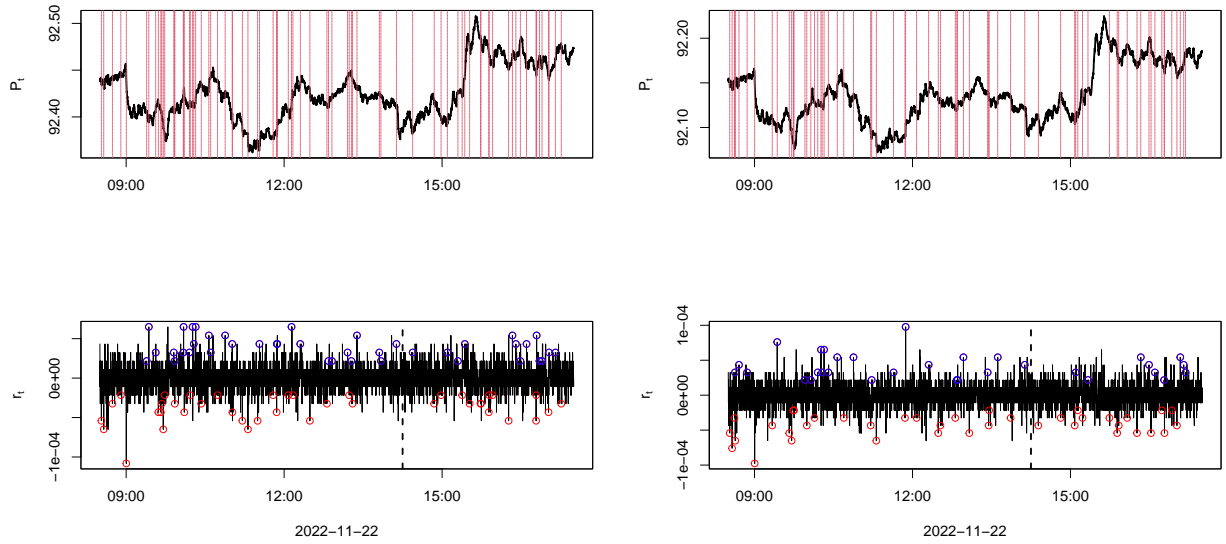


Figure 3: Prices and returns of the green bullet bond issued by Crédit Agricole SA observed at November 22, 2022 (plots on the left refer to ask prices/returns while plots on the right to the bid counterparts). Red and blue circles refer respectively to negative and positive jumps in the series of returns identified through the LM test for $\alpha_{LM} = 0.95$. Vertical red lines in the upper plots refer to time instants where (positive or negative) jumps occur.

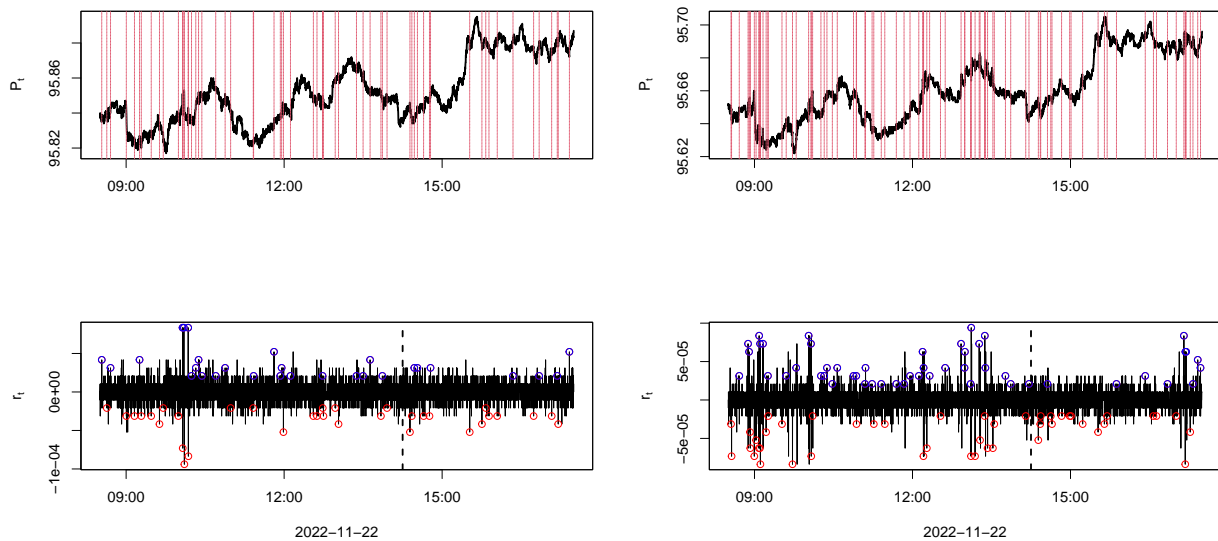


Figure 4: Prices and returns of the brown bullet bond issued by Crédit Agricole SA observed at November 22, 2022 (left ask; right bid). Red and blue circles refer respectively to negative and positive jumps in the series of returns identified through the LM test for $\alpha_{LM} = 0.95$. Vertical red lines in the upper plots refer to time instants where (positive or negative) jumps occur.

Our first attempt is devoted to the fitting of the bivariate CARMA(p,q)-Hawkes model to the counting processes that are made up of any price down or up movement, i.e. framework 1. The residual analysis suggests that the fitting made directly on these two series is not appropriate. We thus consider framework 2 that implies fitting a univariate CARMA(p,q)-Hawkes model to the counting processes obtained applying the LM test to the series of returns for varying levels of the confidence level α_{LM} . Tables 4 and 5 provide the p and q orders of the best fitting univariate CARMA(p,q)-Hawkes models respectively bid and ask prices for the green (bullet and callable) bonds issued by Crédit Agricole SA. The last columns of these tables display the percentage of observations classified as jumps for varying levels of the confidence parameter in the LM test. The results of the selection procedure for the brown (bullet and callable) bonds issued by Crédit Agricole SA are reported respectively in Tables 6 and 7 for bid and ask prices. The corresponding results for green and brown bonds issued by Engie SA are presented respectively in Tables C.10 and C.12. During the trading period August 19-September 12, 2022 only around 4% of observed returns are classified as jumps both for the brown and the green bullet bonds (bid series) while for the series based on ask prices in the case of brown bullet bonds we have 10% of observations classified as jumps. In the second period under investigation, i.e. November 14-December 13, 2022 differences appear between the two categories of bullet bonds issued by Crédit Agricole SA. Indeed, for the case of the green bond less than 5% of observations are classified as jumps while

for the brown bond this quantity is larger than 10% especially in the case of the series based on bid prices. Series based on callable bond prices display totally different patterns as more than half of the observations are classified as jumps.

| α_{LM} | Orders p and q | KS Test (p -value) | % of Jumps |
|---|--------------------|-----------------------|------------|
| <i>Bullet Green coup. 0.375% (Period I)</i> | | | |
| 95% | (1,0) | 0.099 (0.074) | 4.59% |
| 97.5% | (1,0) | 0.098 (0.067) | 4.83% |
| 99% | (1,0) | 0.098 (0.068) | 4.83% |
| 99.5% | (1,0) | 0.098 (0.049) | 5.24% |
| <i>Callable Green coup. 3.95% (Period I)</i> | | | |
| 95% | (1,0) | 0.079 (0.187) | 47.25% |
| 97.5% | (2,0) | 0.042 (0.880) | 49.75% |
| 99% | (1,0) | 0.093 (0.054) | 52.5% |
| 99.5% | (1,0) | 0.097 (0.032) | 54.75% |
| <i>Bullet Green coup. 0.375% (Period II)</i> | | | |
| 95% | (1,0) | 0.073 (0.498) | 3.79% |
| 97.5% | (1,0) | 0.069 (0.534) | 3.93% |
| 99% | (1,0) | 0.064 (0.595) | 4.28% |
| 99% | (2,0) | 0.441 (<0.001) | 4.34% |
| <i>Callable Green coup. 3.95% (Period II)</i> | | | |
| 95% | (2,0) | 0.106 (0.022) | 70.88% |
| 97.5% | (2,0) | 0.132 (0.001) | 76.14% |
| 99% | (2,0) | 0.123 (0.002) | 81.05% |
| 99% | (2,0) | 0.136 (<0.001) | 85.26% |

Table 4: Best fitting CARMA(p,q)-Hawkes models for tick bid prices of green bonds (Bullet and Callable) issued by Crédit Agricole SA observed during two time intervals: August 19-September 19, 2022 (Period I) and November 14 - December 13, 2022 (Period II) for each α_{LM} in the LM test for the identification of jumps. The third and the fourth column refer respectively to the value of the KS test computed on the residuals of the best fitting model (in brackets its p -value) and the rate of observations classified as jumps.

For the cases where the KS fails, we test framework 3 i.e. we split jumps identified through the LM test into positive and negative ones. We then apply the bivariate CARMA(p,q)-Hawkes model to the two counting processes. The results are reported in Tables 8 and 9 for green and brown bonds respectively. We observe that in many cases even this level of deepness of the analysis is not sufficient to produce a statistically significant model that can reproduce our dataset. The opposite happens in the case of the green and brown bonds issued by Engie SA as we are able to find in most of the cases a model that, based on the residual analysis, seems adequate for fit our data (see Tables C.11 and C.13).

| α_{LM} | Orders p and q | KS Test (p -value) | % of Jumps |
|---|----------------|-----------------------|------------|
| <i>Bullet Green coup. 0.375% (Period I)</i> | | | |
| 95% | (1,0) | 0.137 (0.008) | 3.87% |
| 97.5% | (1,0) | 0.143 (0.003) | 4.22% |
| 99% | (1,0) | 0.140 (0.003) | 4.48% |
| 99.5% | (1,0) | 0.139 (0.003) | 4.54% |
| <i>Callable Green coup. 3.95% (Period I)</i> | | | |
| 95% | (1,0) | 0.098 (0.041) | 51.14% |
| 97.5% | (1,0) | 0.093 (0.047) | 54.68% |
| 99% | (2,0) | 0.077 (0.137) | 57.22% |
| 99.5% | (2,1) | 0.048 (0.648) | 60.00% |
| <i>Bullet Green coup. 0.375% (Period II)</i> | | | |
| 95% | (2,0) | 0.366 (<0.001) | 2.64% |
| 97.5% | (2,0) | 0.366 (<0.001) | 2.64% |
| 99% | (2,0) | 0.272 (<0.001) | 2.90% |
| 99.5% | (2,0) | 0.281 (<0.001) | 2.96% |
| <i>Callable Green coup. 3.95% (Period II)</i> | | | |
| 95% | (2,0) | 0.072 (0.275) | 71.33% |
| 97.5% | (2,0) | 0.063 (0.414) | 76.00% |
| 99% | (2,0) | 0.221 (<0.001) | 76.41% |
| 99.5% | (2,0) | 0.162 (<0.001) | 80.28% |

Table 5: Best fitting CARMA(p,q)-Hawkes models for tick ask prices of green bonds (bullet and callable) issued by Crédit Agricole SA observed during two time intervals: August 19-September 19, 2022 (Period I) and November 14 - December 13, 2022 (Period II) for each α_{LM} in the LM test for the identification of jumps. The third and the fourth column refer respectively to the value of the KS test computed on the residuals of the best fitting model (in brackets its p -value) and the rate of observations classified as jumps.

| α_{LM} | Orders p and q | KS Test (p -value) | % of Jumps |
|---|--------------------|-----------------------|------------|
| <i>Bullet Brown coup. 0.5% (Period I)</i> | | | |
| 95% | (1,0) | 0.064 (0.524) | 4.47% |
| 97.5% | (1,0) | 0.067 (0.418) | 4.83% |
| 99% | (1,0) | 0.064 (0.412) | 5.3% |
| 99.5% | (1,0) | 0.065 (0.357) | 5.54% |
| <i>Callable Brown coup. 3.8% (Period I)</i> | | | |
| 95% | (1,0) | 0.102 (0.091) | 42.74% |
| 97.5% | (2,0) | 0.103 (0.072) | 45.30% |
| 99% | (1,0) | 0.109 (0.040) | 47.29% |
| 99.5% | (2,0) | 0.076 (0.257) | 50.43% |
| <i>Bullet Brown Bond coup. 0.5% (Period II)</i> | | | |
| 95% | (2,0) | 0.043 (0.255) | 16.24% |
| 97.5% | (2,0) | 0.039 (0.310) | 16.87% |
| 99% | (2,0) | 0.036 (0.394) | 17.42% |
| 99.5% | (2,0) | 0.042 (0.225) | 17.94% |
| <i>Callable Brown coup. 3.8% (Period II)</i> | | | |
| 95% | (2,0) | 0.185 (<0.001) | 72.08% |
| 97.5% | (2,0) | 0.192 (<0.001) | 74.11% |
| 99% | (2,0) | 0.208 (<0.001) | 78.17% |
| 99.5% | (2,0) | 0.194 (<0.001) | 79.7% |

Table 6: Best fitting CARMA(p,q)-Hawkes models for tick bid prices of brown bonds (bullet and callable) issued by Crédit Agricole SA observed during two time intervals: August 19-September 19, 2022 (Period I) and November 14 - December 13, 2022 (Period II) for each α_{LM} in the LM test for the identification of jumps. The third and the fourth column refer respectively to the value of the KS test computed on the residuals of the best fitting model (in brackets its p -value) and the rate of observations classified as jumps.

| α_{LM} | Orders p and q | KS Test (p -value) | % of Jumps |
|--|--------------------|-----------------------|------------|
| <i>Bullet Brown coup. 0.5% (Period I)</i> | | | |
| 95% | (1,0) | 0.069 (0.070) | 9.88% |
| 97.5% | (1,0) | 0.068 (0.062) | 10.32% |
| 99% | (1,0) | 0.071 (0.039) | 10.79% |
| 99.5% | (1,0) | 0.071 (0.038) | 11.01% |
| <i>Callable Brown coup. 3.8% (Period I)</i> | | | |
| 95% | (2,0) | 0.037 (0.965) | 50.28% |
| 97.5% | (2,1) | 0.032 (0.992) | 51.69% |
| 99% | (1,0) | 0.079 (0.180) | 54.24% |
| 99.5% | (1,0) | 0.084 (0.129) | 55.65% |
| <i>Bullet Brown coup. 0.5% (Period II)</i> | | | |
| 95% | (1,0) | 0.046 (0.388) | 11.63% |
| 97.5% | (1,0) | 0.050 (0.282) | 11.96% |
| 99% | (2,0) | 0.031 (0.812) | 12.32% |
| 99.5% | (2,0) | 0.032 (0.783) | 12.44% |
| <i>Callable Brown coup. 3.8% (Period II)</i> | | | |
| 95% | (2,0) | 0.126 (0.022) | 66.82% |
| 97.5% | (2,0) | 0.147 (0.003) | 70.09% |
| 99% | (2,1) | 0.123 (0.020) | 71.96% |
| 99.5% | (2,1) | 0.054 (0.746) | 73.83% |

Table 7: Best fitting CARMA(p,q)-Hawkes models for a dataset based on tick ask prices of brown bonds (bullet and callable) issued by Crédit Agricole SA observed during two time intervals: August 19-September 19, 2022 (Period I) and November 14 - December 13, 2022 (Period II) for each α_{LM} in the LM test for the identification of jumps. The third and the fourth column refer respectively to the value of the KS test computed on the residuals of the best fitting model (in brackets its p -value) and the rate of observations classified as jumps.

| α_{LM} | Orders p and q | KS ₁ (p-value) | KS ₂ (p-value) |
|---------------|---|---------------------------|---------------------------|
| | <i>Bullet Green coup. 0.375% (Period I) Bid</i> | | |
| 99.5% | (1, 1, 0, 0, 0) | 0.142 (0.154) | 0.065 (0.859) |
| | <i>Callable Green coup. 3.95% (Period I) Bid</i> | | |
| 99.5% | (2, 2, 1, 0, 1, 0) | 0.074 (0.546) | 0.065 (0.735) |
| | <i>Callable Green coup. 3.95% (Period II) Bid</i> | | |
| 95% | (2, 2, 1, 0, 0, 0) | 0.116 (0.056) | 0.354 (2.34e-08) |
| 97.5% | (2, 2, 1, 0, 0, 0) | 0.138 (0.008) | 0.129 (0.145) |
| 99% | (2, 2, 1, 0, 0, 0) | 0.097 (0.117) | 0.116 (0.196) |
| 99.5% | (2, 1, 1, 0, 1, 0) | 0.119 (0.024) | 0.093 (0.406) |
| | <i>Callable Green coup. 3.95% (Period I) Ask</i> | | |
| 97.5% | (2, 2, 0, 0, 0, 0) | 0.061 (0.825) | 0.079 (0.519) |
| | <i>Bullet Green coup. 0.375%(Period II) Ask</i> | | |
| 97.5% | (2, 2, 1, 1, 1, 1) | 0.177 (0.011) | 0.109 (0.32) |
| 99% | (2, 1, 1, 1, 0, 0) | 0.171 (0.0132) | 0.135 (0.097) |
| 99.5% | (2, 2, 1, 1, 1, 1) | 0.194 (0.003) | 0.099 (0.369) |
| | <i>Bullet Green coup. 0.375%(Period II) Ask</i> | | |
| 95% | (1, 1, 0, 0, 0, 0) | 0.103 (0.691) | 0.162 (0.196) |
| 97.5% | (1, 1, 0, 0, 0, 0) | 0.103 (0.691) | 0.162 (0.196) |
| 99% | (1, 1, 0, 0, 0, 0) | 0.154 (0.159) | 0.143 (0.285) |
| 99.5% | (1, 1, 0, 0, 0, 0) | 0.179 (0.064) | 0.121 (0.459) |
| | <i>Callable Green coup. 3.95% (Period II) Ask</i> | | |
| 99% | (2, 2, 1, 0, 0, 1) | 0.115 (0.060) | 0.148 (0.062) |
| 99.5% | (2, 2, 1, 0, 0, 1) | 0.099 (0.126) | 0.119 (0.178) |

Table 8: Results for a bivariate CARMA(p,q)-Hawkes model as specified in framework 3 presented in Section 2.1 fitted to a set tick ask prices of green bonds (bullet and callable) issued by Crédit Agricole SA observed during two time intervals: August 19-September 19, 2022 (Period I) and November 14 - December 13, 2022 (Period II) for the levels of α_{LM} in the LM test. The third and the fourth column refer respectively to the value of the KS test computed on the residuals (in brackets its p -value) from the set of upward and downward jumps.

| α_{LM} | Orders p and q | KS ₁ (p-value) | KS ₂ (p-value) |
|---------------|---|---------------------------|---------------------------|
| | <i>Callable Brown Bond - (Period I) - coupon rate 3.8% Bid</i> | | |
| 99% | (2, 2, 1, 0, 0, 1) | 0.067 (0.764) | 0.099 (0.381) |
| | <i>Callable Brown Bond - (Period II) - coupon rate 3.8% Bid</i> | | |
| 95% | (2, 2, 1, 0, 0, 0) | 0.116 (0.226) | 0.146 (0.178) |
| 97.5% | (2, 2, 0, 0, 0, 0) | 0.089 (0.510) | 0.155 (0.110) |
| 99% | (2, 2, 0, 0, 0, 0) | 0.090 (0.462) | 0.153 (0.109) |
| 99.5% | (2, 2, 1, 0, 0, 0) | 0.114 (0.194) | 0.154 (0.091) |
| | <i>Bullet Brown Bond - (Period I) - coupon rate 0.5%</i> | | |
| 99% | (2, 1, 1, 0, 1, 0) | 0.219 (<0.001) | 0.070 (0.287) |
| 99.5% | (2, 1, 1, 0, 1, 0) | 0.276 (<0.001) | 0.1697 (<0.001) |
| | <i>Callable Brown Bond - (Period II) - coupon rate 3.8% Ask</i> | | |
| 95% | (2, 2, 1, 0, 0, 0) | 0.064 (0.872) | 0.155 (0.157) |
| 97.5% | (2, 2, 0, 0, 0, 0) | 0.072 (0.728) | 0.149 (0.163) |
| 99% | (2, 2, 0, 0, 0, 0) | 0.132 (0.077) | 0.170 (0.070) |

Table 9: Results for a bivariate CARMA(p,q)-Hawkes model as specified in framework 3 presented in Section 2.1 fitted to a set tick ask prices of brown bonds (bullet and callable) issued by Crédit Agricole SA observed during two time intervals: August 19-September 19, 2022 (Period I) and November 14 - December 13, 2022 (Period II) for the levels of α_{LM} in the LM test. The third and the fourth column refer respectively to the value of the KS Test computed on the residuals (in brackets its p -value) from the set of upward and downward jumps.

4. Conclusions

In this paper we investigated market activity of bonds through the introduction of a bivariate model for the intensity of positive and negative jumps in a high frequency framework where we allow for a non-monotonic vanishing effect of jumps. We considered both ask and bid prices where we identified the best fitting models for brown and green bonds. This study dealt both with bullet and callable bonds as we expected these two instruments to behave differently when observed at the lens of trading activity. Results suggest that the bid-ask spread of green bonds is larger on average, especially during autumn. Moreover, higher order CARMA(p,q)-Hawkes models seem to be useful in order to reproduce the sequence of jumps.

References

- [1] B. Hachenberg, D. Schiereck, Are green bonds priced differently from conventional bonds?, *Journal of Asset Management* 19 (6) (2018) 371–383.
- [2] M. J. Bachelet, L. Becchetti, S. Manfredonia, The green bonds premium puzzle: The role of issuer characteristics and third-party verification, *Sustainability* 11 (4) (2019) 1098.
- [3] M. Baker, D. Bergstresser, G. Serafeim, J. Wurgler, Financing the response to climate change: The pricing and ownership of US green bonds, Tech. rep., National Bureau of Economic Research (2018).
- [4] J. C. Reboredo, Green bond and financial markets: Co-movement, diversification and price spillover effects, *Energy Economics* 74 (2018) 38–50.
- [5] L. Pham, T. L. D. Huynh, How does investor attention influence the green bond market?, *Finance Research Letters* 35 (2020) 101533.
- [6] M. Martiradonna, S. Romagnoli, A. Santini, The beneficial role of green bonds as a new strategic asset class: Dynamic dependencies, allocation and diversification before and during the pandemic era, *Energy Economics* (2023) 106587.
- [7] K. Sohag, M. K. Hassan, S. Bakhteyev, O. Mariev, Do green and dirty investments hedge each other?, *Energy Economics* 120 (2023) 106573.
- [8] A. Pietsch, D. Salakhova, Pricing of green bonds: drivers and dynamics of the greenium, Working paper (2022).
- [9] B. Biais, R. Green, The microstructure of the bond market in the 20th century, *Review of Economic Dynamics* 33 (2019) 250–271.
- [10] H. Bessembinder, C. Spatt, K. Venkataraman, A survey of the microstructure of fixed-income markets, *Journal of Financial and Quantitative Analysis* 55 (1) (2020) 1–45.
- [11] S. S. Lee, P. A. Mykland, Jumps in financial markets: A new nonparametric test and jump dynamics, *The Review of Financial Studies* 21 (6) (2008) 2535–2563.
- [12] A.-M. Dumitru, G. Urga, Identifying jumps in financial assets: a comparison between nonparametric jump tests, *Journal of Business & Economic Statistics* 30 (2) (2012) 242–255.
- [13] R. Brignone, L. Gonzato, C. Sgarra, Commodity Asian option pricing and simulation in a 4-factor model with jump clusters, *Annals of Operations Research* (2023) 1–32.
- [14] X. Li, Y. Liao, X. Lu, F. Ma, An oil futures volatility forecast perspective on the selection of -frequency jump tests, *Energy Economics* 116 (2022) 106358.
- [15] L. Mercuri, A. Perchiazzo, E. Rroji, A Hawkes model with CARMA (p,q) intensity, arXiv preprint arXiv:2208.02659 (2022).
- [16] E. Bacry, I. Mastromatteo, J.-F. Muzy, Hawkes processes in finance, *Market Microstructure and Liquidity* 1 (01) (2015) 1550005.

- [17] J. Da Fonseca, R. Zaatour, Hawkes process: Fast calibration, application to trade clustering, and diffusive limit, *Journal of Futures Markets* 34 (6) (2014) 548–579.
- [18] K. Boudt, O. Kleen, E. Sjørup, Analyzing Intraday Financial Data in R: The highfrequency Package, *Journal of Statistical Software* 104 (2022) 1–36.
- [19] M. Kendall, A. Stuart, *The advanced theory of statistics. vol. 1: Distribution theory*, London: Griffin (1977).
- [20] E. N. Brown, R. Barbieri, V. Ventura, R. E. Kass, L. M. Frank, The time-rescaling theorem and its application to neural spike train data analysis, *Neural computation* 14 (2) (2002) 325–346.

Appendix A. Likelihood function

The solution of $d\mathbf{X}_t = \mathbf{A}\mathbf{X}_t dt + \mathbf{e}d\mathbf{N}_t$, with $\mathbf{X}_0 = \mathbf{0}$ (linear SDE) is given as in (6) and substituting it in the first integral of (12), the likelihood function can be rewritten as

$$\begin{aligned}
\mathcal{L} &= -\mathbb{1}^\top \boldsymbol{\mu} (T - 0) - \mathbb{1}^\top \mathbf{B} \int_0^T \left[\int_0^t e^{\mathbf{A}(t-s)} \mathbf{e} d\mathbf{N}_s \right] dt + \sum_{T_k \leq T} \ln (\boldsymbol{\mu} + \mathbf{B}\mathbf{X}_{T_k})^\top \Delta \mathbf{N}_{T_k} \\
&= -\mathbb{1}^\top \boldsymbol{\mu} T - \mathbb{1}^\top \mathbf{B} \int_0^T \mathbf{A}^{-1} \left[e^{\mathbf{A}(T-s)} - \mathbf{I} \right] \mathbf{e} d\mathbf{N}_s + \sum_{T_k \leq T} \ln (\boldsymbol{\mu} + \mathbf{B}\mathbf{X}_{T_k})^\top \Delta \mathbf{N}_{T_k} \\
&= -\mathbb{1}^\top \boldsymbol{\mu} T - \mathbb{1}^\top \mathbf{B} \mathbf{A}^{-1} \sum_{T_k \leq T} e^{\mathbf{A}(T-T_k)} \mathbf{e} \Delta \mathbf{N}_{T_k} + \mathbb{1}^\top \mathbf{B} \mathbf{A}^{-1} \mathbf{e} \sum_{T_k \leq T} \Delta \mathbf{N}_{T_k} \\
&\quad + \sum_{T_k \leq T} \ln (\boldsymbol{\mu} + \mathbf{B}\mathbf{X}_{T_k})^\top \Delta \mathbf{N}_{T_k}
\end{aligned}$$

where $\mathbb{1}^\top \mathbf{B} \mathbf{A}^{-1} \mathbf{e} \sum_{T_k \leq T} \Delta \mathbf{N}_{T_k} = \mathbb{1}^\top \mathbf{B} \mathbf{A}^{-1} \mathbf{e} \mathbf{N}_T$. Therefore the likelihood function becomes

$$\mathcal{L} = -\mathbb{1}^\top \boldsymbol{\mu} T + \mathbb{1}^\top \mathbf{B} \mathbf{A}^{-1} \mathbf{e} \mathbf{N}_T - \mathbb{1}^\top \mathbf{B} \mathbf{A}^{-1} \sum_{T_k \leq T} e^{\mathbf{A}(T-T_k)} \mathbf{e} \Delta \mathbf{N}_{T_k} + \sum_{T_k \leq T} \ln (\boldsymbol{\mu} + \mathbf{B}\mathbf{X}_{T_k})^\top \Delta \mathbf{N}_{T_k}. \quad (\text{A.1})$$

If we observe n jumps in $[0, T]$, $\sum_{T_k \leq T} e^{\mathbf{A}(T-T_k)} \mathbf{e} \Delta \mathbf{N}_{T_k} = e^{\mathbf{A}(T-T_n)} \sum_{k=1}^n e^{\mathbf{A}(T_n-T_k)} \mathbf{e} \Delta \mathbf{N}_{T_k}$ and define

$$s(n) = \sum_{k=1}^n e^{\mathbf{A}(T_n-T_k)} \mathbf{e} \Delta \mathbf{N}_{T_k}, \quad (\text{A.1}) \text{ reads}$$

$$\mathcal{L} = -\mathbb{1}^\top \boldsymbol{\mu} T + \mathbb{1}^\top \mathbf{B} \mathbf{A}^{-1} \mathbf{e} \mathbf{N}_T - \mathbb{1}^\top \mathbf{B} \mathbf{A}^{-1} e^{\mathbf{A}(T-T_n)} s(n) + \sum_{i=1}^n \ln (\boldsymbol{\mu} + \mathbf{B}\mathbf{X}_{T_i})^\top \Delta \mathbf{N}_{T_i}. \quad (\text{A.2})$$

The final expression of the likelihood function is explicit assuming that $T = T_n$ i.e. we have n jumps in $[0, T_n]$.

Appendix B. Estimation procedure

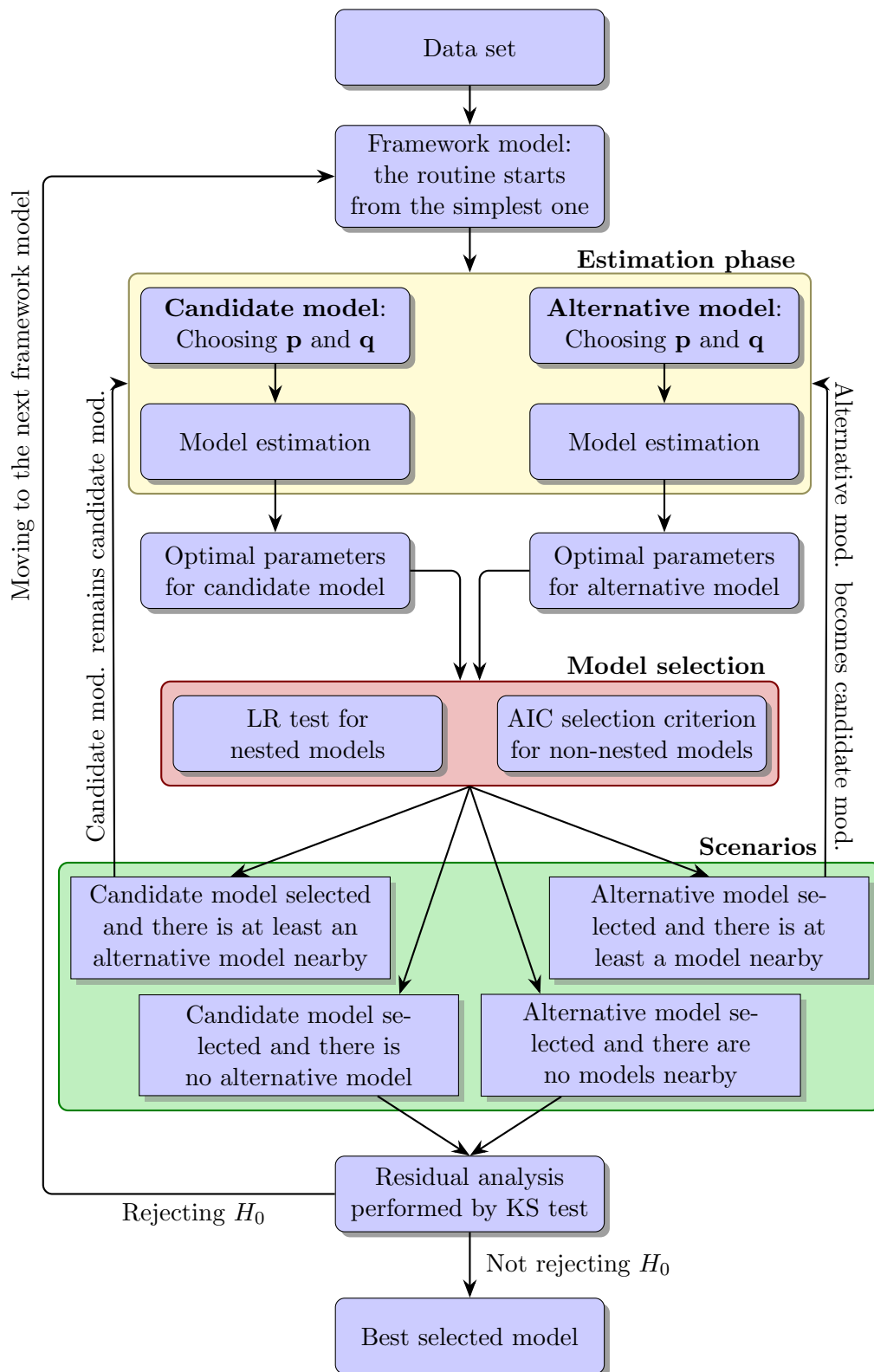


Figure B.5: Description for the analysis of the microstructure for a given time series of bond prices. The three alternative frameworks are 1) The bivariate CARMA(p,q)-Hawkes applied to jumps identified at any price movement 2) The Univariate CARMA(p,q)-Hawkes model applied to all the jumps identified through the LM test and 3) The bivariate CARMA(p,q)-Hawkes applied to positive and negative jumps identified through the LM test.

Appendix C. Results for callable and corporate bonds

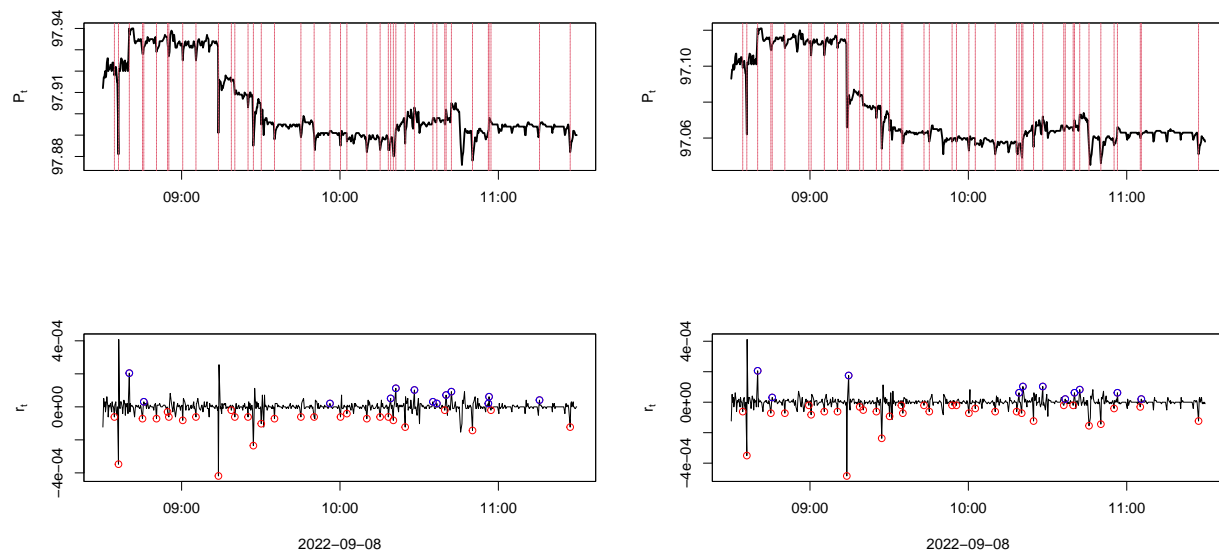


Figure C.6: Prices and returns of the green callable bond issued by Crédit Agricole SA observed at September 8, 2022 (left ask; right bid). Red and blue circles refer respectively to negative and positive jumps in the series of returns identified through the LM test for $\alpha_{LM} = 0.95$. Vertical red lines in the upper plots refer to time instants where (positive or negative) jumps occur.

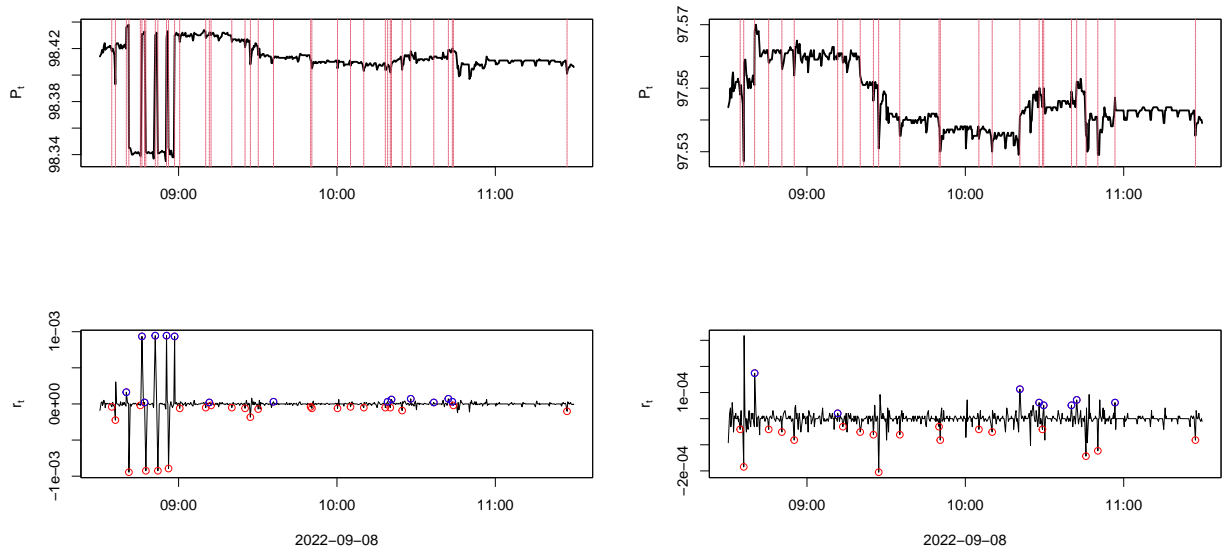


Figure C.7: Prices and returns of the brown callable bond issued by Crédit Agricole SA observed at September 8, 2022 (left ask; right bid). Red and blue circles refer respectively to negative and positive jumps in the series of returns identified through the LM test for $\alpha_{LM} = 0.95$. Vertical red lines in the upper plots refer to time instants where (positive or negative) jumps occur.

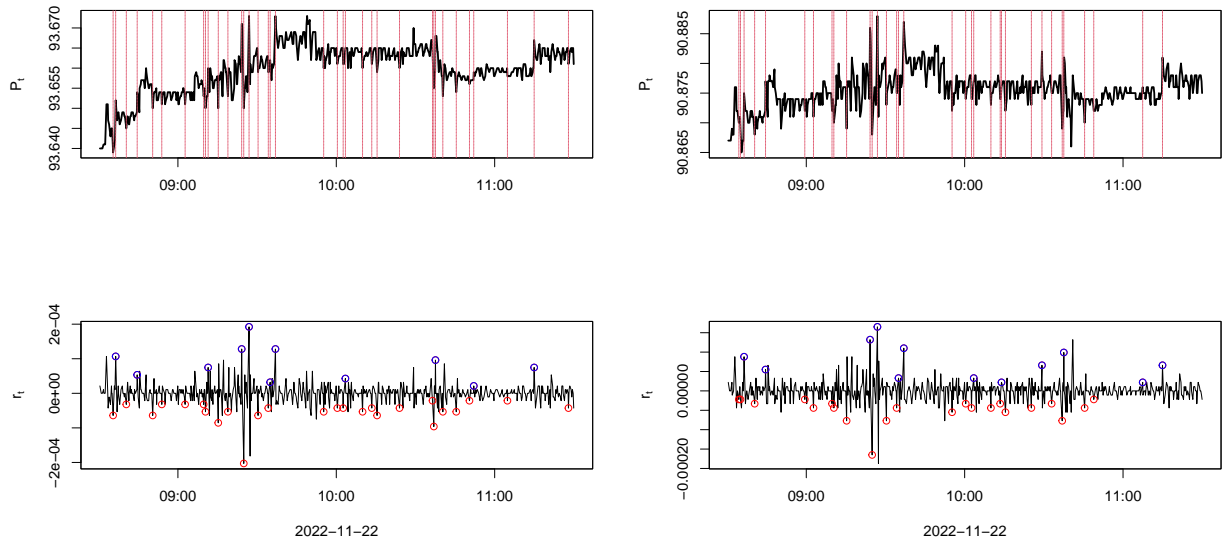


Figure C.8: Prices and returns of the green callable bond issued by Crédit Agricole SA observed at November 22, 2022 (left ask; right bid). Red and blue circles refer respectively to negative and positive jumps in the series of returns identified through the LM test for $\alpha_{LM} = 0.95$. Vertical red lines in the upper plots refer to time instants where (positive or negative) jumps occur.

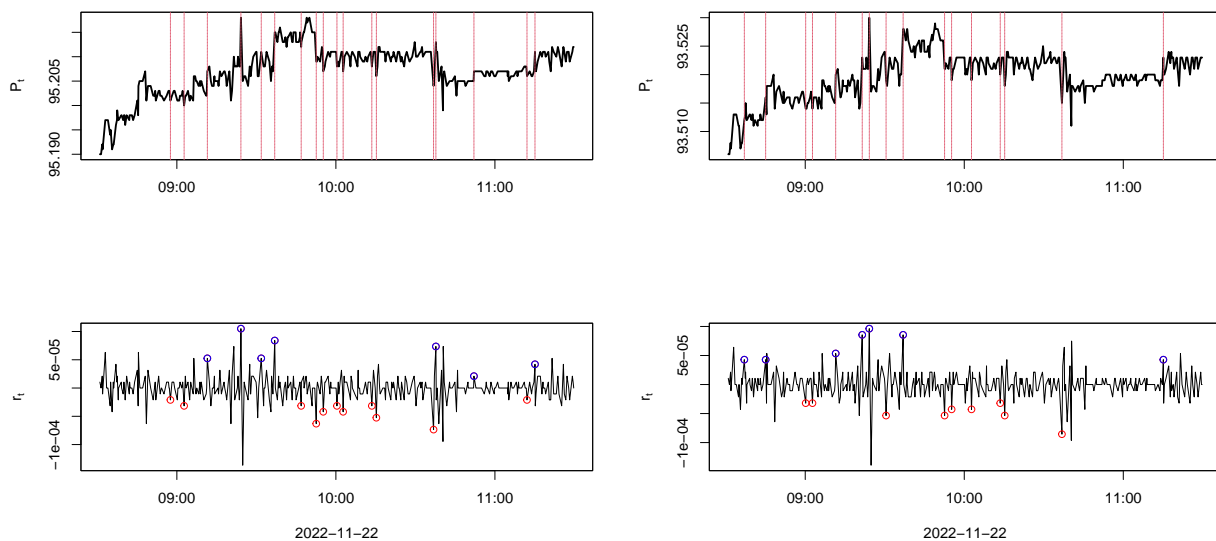


Figure C.9: Prices and returns of the brown callable bond issued by Crédit Agricole SA observed at November 22, 2022 (plots on the left refer to ask prices/returns while plots on the right to the bid counterparts). Red and blue circles refer respectively to negative and positive jumps in the series of returns identified through the LM test for $\alpha_{LM} = 0.95$. Vertical red lines in the upper plots refer to time instants where (positive or negative) jumps occur.

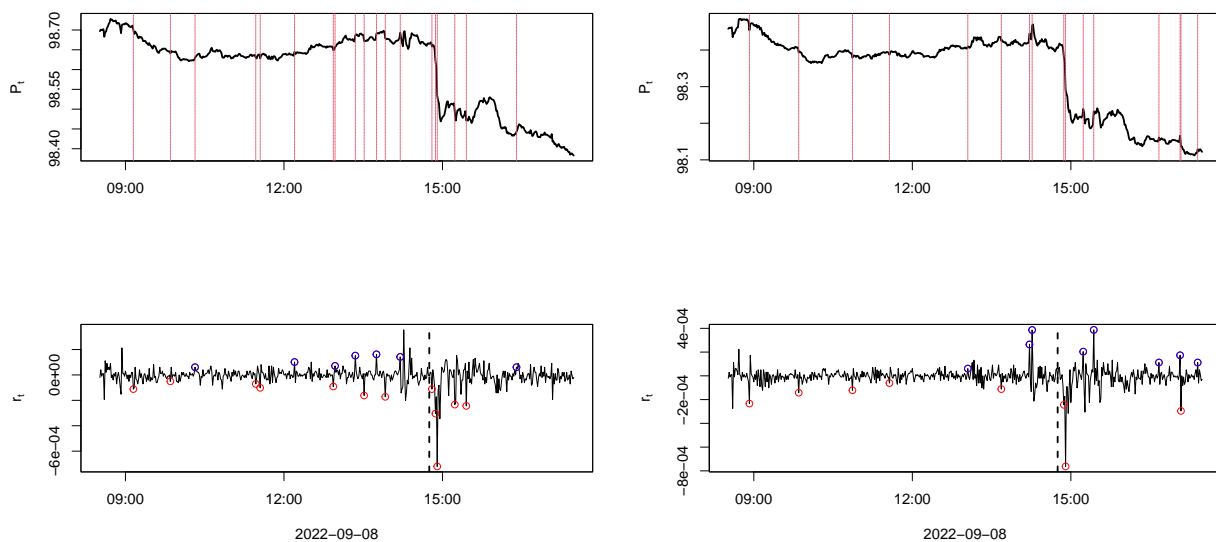


Figure C.10: Prices and returns of the green bullet bond issued by Engie SA observed at September 8, 2022 (plots on the left refer to ask prices/returns while plots on the right to the bid counterparts). Red and blue circles refer respectively to negative and positive jumps in the series of returns identified through the LM test for $\alpha_{LM} = 0.95$. Vertical red lines in the upper plots refer to time instants where (positive or negative) jumps occur.

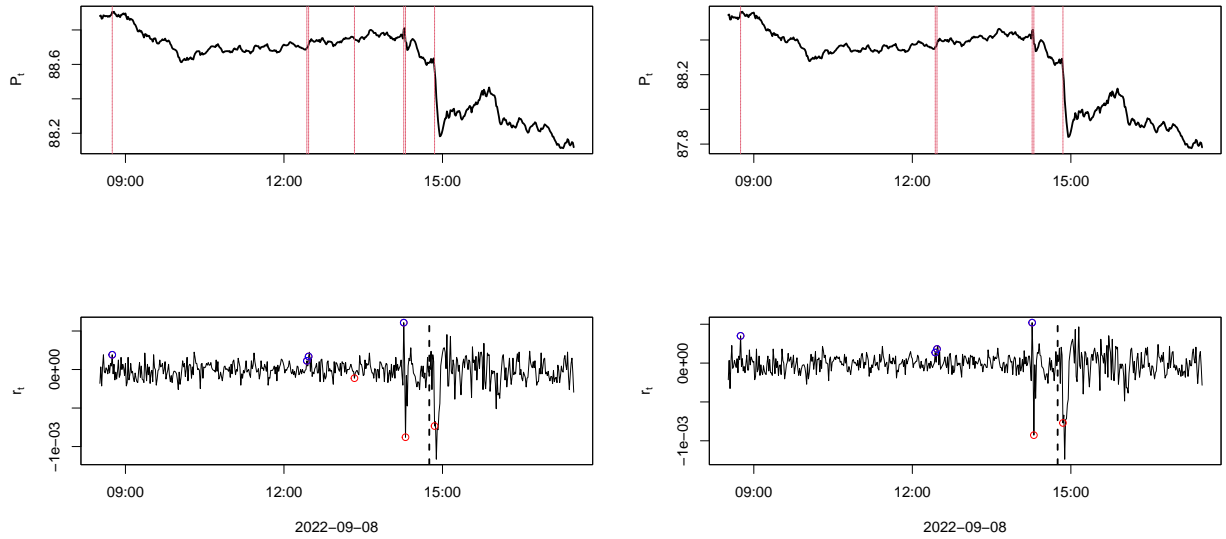


Figure C.11: Prices and returns of the brown bullet bond issued by Engie SA observed at September 8, 2022 (plots on the left refer to ask prices/returns while plots on the right to the bid counterparts). Red and blue circles refer respectively to negative and positive jumps in the series of returns identified through the LM test for $\alpha_{LM} = 0.95$. Vertical red lines in the upper plots refer to time instants where (positive or negative) jumps occur.

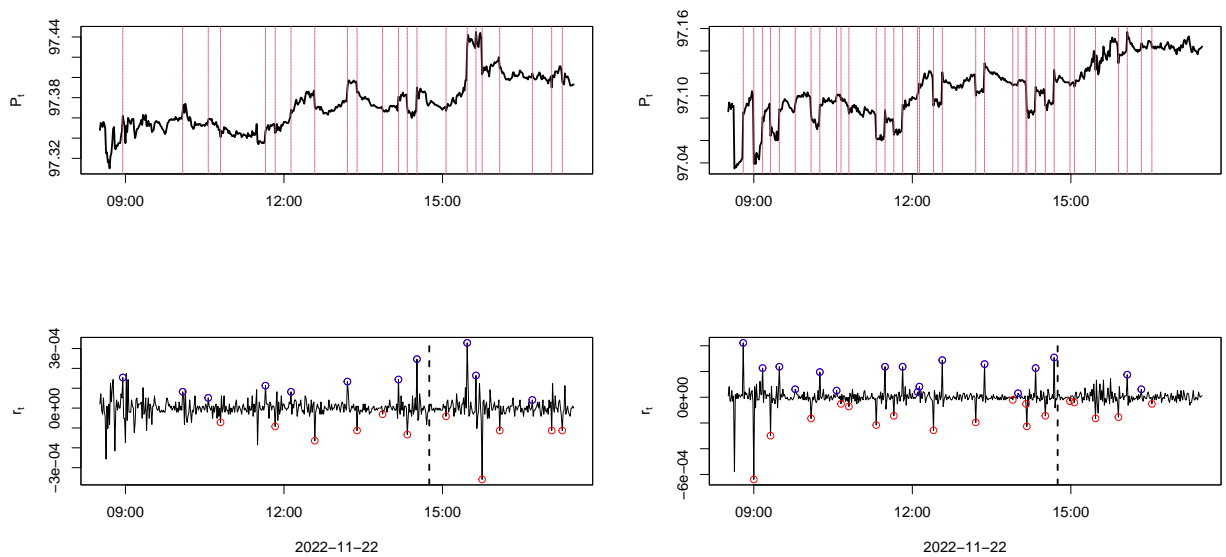


Figure C.12: Prices and returns of the green bullet bond issued by Engie SA observed at November 22, 2022 (left ask; right bid). Red and blue circles refer respectively to negative and positive jumps in the series of returns identified through the LM test for $\alpha_{LM} = 0.95$. Vertical red lines in the upper plots refer to time instants where (positive or negative) jumps occur.

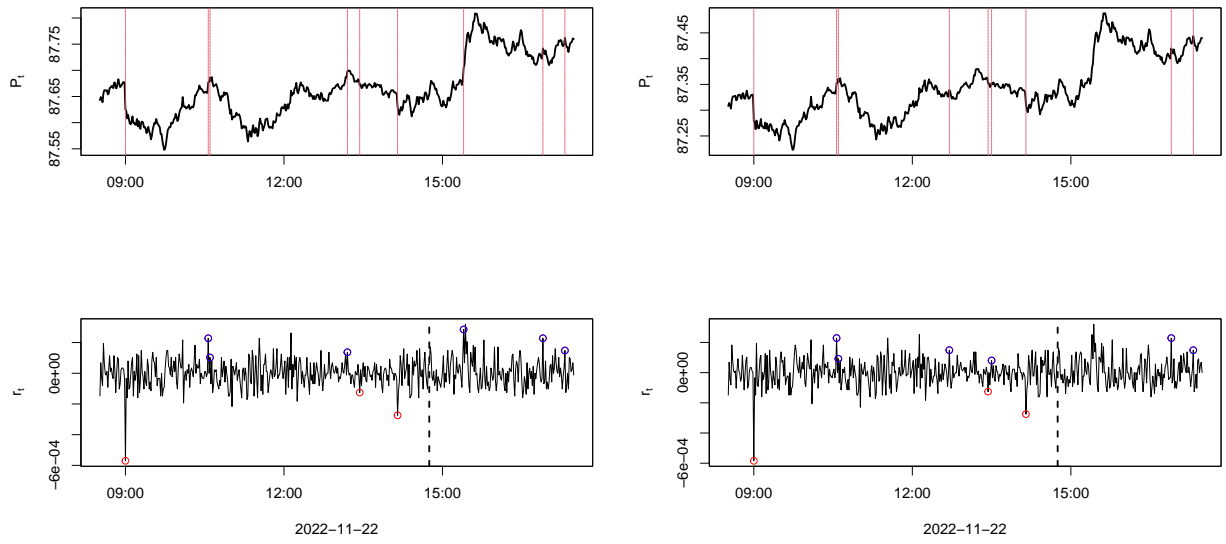


Figure C.13: Prices and returns of the brown bullet bond issued by Engie SA observed at November 22, 2022 (left ask; right bid). Red and blue circles refer respectively to negative and positive jumps in the series of returns identified through the LM test for $\alpha_{LM} = 0.95$. Vertical red lines in the upper plots refer to time instants where (positive or negative) jumps occur.

| α_{LM} | Orders p and q | KS Test (p -value) | % of Jumps |
|--|----------------|-----------------------|------------|
| <i>Bullet Green coup. 0.875% (Period I) Ask</i> | | | |
| 95% | (2,0) | 0.129 (0.010) | 35.29% |
| 97.5% | (2,1) | 0.111 (0.028) | 38.34% |
| 99% | (2,1) | 0.069 (0.309) | 42.48% |
| 99.5% | (2,1) | 0.056 (0.547) | 44.01% |
| <i>Bullet Green coup. 0.875% (Period I) Bid</i> | | | |
| 95% | (2,0) | 0.053 (0.474) | 58.64% |
| 97.5% | (2,1) | 0.076 (0.085) | 63.18% |
| 99% | (2,0) | 0.057 (0.298) | 65.68% |
| 99.5% | (2,0) | 0.049 (0.472) | 68.18% |
| <i>Bullet Green coup. 0.875% (Period II) Ask</i> | | | |
| 95% | (1,0) | 0.073 (0.165) | 54.80% |
| 97.5% | (2,1) | 0.050 (0.567) | 57.85% |
| 99% | (2,0) | 0.035 (0.909) | 62.30% |
| 99.5% | (2,0) | 0.032 (0.941) | 64.40% |
| <i>Bullet Green coup. 0.875% (Period II) Bid</i> | | | |
| 95% | (2,1) | 0.046 (0.521) | 76.47% |
| 97.5% | (2,1) | 0.044 (0.559) | 77.94% |
| 99% | (2,1) | 0.049 (0.415) | 81.13% |
| 99.5% | (2,1) | 0.053 (0.309) | 82.60% |

Table C.10: Best fitting CARMA(p,q)-Hawkes models for tick ask and bid prices of green bullet bonds issued by Engie SA observed during two time intervals: August 19-September 19, 2022 (Period I) and November 14 - December 13, 2022 (Period II) for each α_{LM} in the LM test for the identification of jumps. The third and the fourth column refer respectively to the value of the KS test computed on the residuals of the best fitting model (in brackets its p -value) and the rate of observations classified as jumps.

| α_{LM} | Orders p and q | KS ₁ (p -value) | KS ₂ (p -value) |
|---|--------------------|-------------------------------|-------------------------------|
| <i>Bullet Green coup. 0.875% (Period I) Ask</i> | | | |
| 95% | (2, 2, 0, 0, 0, 0) | 0.059 (0.911) | 0.070 (0.838) |
| 97.5% | (2, 2, 0, 0, 0, 0) | 0.077 (0.643) | 0.079 (0.638) |

Table C.11: Results for a bivariate CARMA(p,q)-Hawkes model as specified in framework 3 presented in Section 2.1 fitted to a set of tick bid and ask prices of green bullet bonds issued by Engie SA observed during two time intervals: August 19-September 19, 2022 (Period I) and November 14 - December 13, 2022 (Period II) for the levels of α_{LM} in the LM test. The third and the fourth column refer respectively to the value of the KS test computed on the residuals (in brackets its p -value) from the set of upward and downward jumps.

| α_{LM} | Orders p and q | KS Test (p -value) | % of Jumps |
|--|----------------|-----------------------|------------|
| <i>Bullet Brown coup. 0.375% (Period I) Ask</i> | | | |
| 95% | (1,0) | 0.064 (0.861) | 16.73% |
| 97.5% | (1,0) | 0.057 (0.911) | 18.53% |
| 99% | (1,0) | 0.067 (0.757) | 20.12% |
| 99.5% | (2,0) | 0.387 (<0.001) | 22.31% |
| <i>Bullet Brown coup. 0.375% (Period I) Bid</i> | | | |
| 95% | (2,0) | 0.365 (<0.001) | 20.28% |
| 97.5% | (2,0) | 0.387 (<0.001) | 22.24% |
| 99% | (1,0) | 0.074 (0.518) | 24.21% |
| 99.5% | (1,0) | 0.089 (0.250) | 25.98% |
| <i>Bullet Brown coup. 0.375% (Period II) Ask</i> | | | |
| 95% | (1,0) | 0.095 (0.2888) | 21.34% |
| 97.5% | (2,0) | 0.432 (<0.001) | 23.72% |
| 99% | (2,0) | 0.438 (<0.001) | 27.27% |
| 99.5% | (1,0) | 0.091 (0.1701) | 29.84% |
| <i>Bullet Brown coup. 0.375% (Period II) Bid</i> | | | |
| 95% | (1,0) | 0.088 (0.330) | 22.90% |
| 97.5% | (2,0) | 0.403 (<0.001) | 25.24% |
| 99% | (2,0) | 0.481 (<0.001) | 27.40% |
| 99.5% | (1,0) | 0.069 (0.466) | 29.55% |

Table C.12: Best fitting CARMA(p,q)-Hawkes models for tick ask and bid prices of brown bullet bonds issued by Engie SA observed during two time intervals: August 19-September 19, 2022 (Period I) and November 14 - December 13, 2022 (Period II) for each α_{LM} in the LM test for the identification of jumps. The third and the fourth column refer respectively to the value of the KS test computed on the residuals of the best fitting model (in brackets its p -value) and the rate of observations classified as jumps.

| α_{LM} | Orders p and q | KS ₁ (p -value) | KS ₂ (p -value) |
|--|--------------------|-------------------------------|-------------------------------|
| <i>Bullet Brown coup. 0.375% (Period I) Ask</i> | | | |
| 99.5% | (2, 1, 0, 0, 0, 0) | 0.111 (0.464) | 0.246 (0.003) |
| <i>Bullet Brown coup. 0.375% (Period I) Bid</i> | | | |
| 95% | (2, 1, 0, 0, 0, 0) | 0.117 (0.406) | 0.118 (0.550) |
| 97.5% | (2, 1, 1, 0, 0, 0) | 0.072 (0.891) | 0.101 (0.677) |
| <i>Bullet Brown coup. 0.375% (Period II) Ask</i> | | | |
| 97.5% | (2, 1, 1, 0, 1, 0) | 0.143 (0.127) | 0.128 (0.344) |
| 99% | (2, 1, 1, 0, 1, 0) | 0.122 (0.182) | 0.232 (0.004) |
| <i>Bullet Brown coup. 0.375% (Period II) Bid</i> | | | |
| 97.5% | (2, 1, 1, 0, 0, 0) | 0.140 (0.113) | 0.066 (0.960) |
| 99% | (2, 1, 1, 0, 0, 0) | 0.043 (0.997) | 0.160 (0.103) |

Table C.13: Results for a bivariate CARMA(p,q)-Hawkes model as specified in framework 3 presented in Section 2.1 fitted to a set of tick ask and bid prices of brown bullet bonds issued by Engie SA observed during two time intervals: August 19-September 19, 2022 (Period I) and November 14 - December 13, 2022 (Period II) for the levels of α_{LM} in the LM test. The third and the fourth column refer respectively to the value of the KS test computed on the residuals (in brackets its p -value) from the set of upward and downward jumps.